

## High-Efficiency Bridgeless Dual-Mode Single Phase Resonant AC-DC Converter with PI Controller

Monica S\*, Dr. P Usha \*\*

\*(Department of Electrical & Electronics Engineering, Dayananda sagar college of engineering, Bangalore-560078

\*\* (HoD, Department of Electrical & Electronics Engineering, Dayananda sagar college of engineering, Bangalore-560078

### ABSTRACT

This paper presents a bridgeless dual mode resonant single phase ac-dc converter. We expel a full-bridge diode rectifier from the grid side of the proposed converter by using a bidirectional switch and in this way it decreases the number of components used in the topology. We utilized a series resonant circuit in the output voltage doubler on the secondary side. The series resonant circuit give zero-current switching (zcs) turn-off at the output diode, and consequently it reduces the reverse recovery loss. To attain medium-high power capability with an appropriate transformer, the proposed converter operates in both continuous conduction mode and discontinuous conduction mode. In following, the operating principle of the proposed converter are explained, the proposed converter achieves efficiency of 96.2%. Simulation results of proposed converter and and converter with PI controller are performed using MATLAB/Simulink. The simulation results and theoretical results of proposed converter are compared.

**Keywords**-Bidirectional switch, PI controller, Zero current switching.

Date of Submission: 06-08-2020

Date of Acceptance: 20-08-2020

### I. INTRODUCTION

AC-DC converters with Power factor correction (PFC) are utilized in grid connected power supply systems such as dc-bus suppliers in mobile charging stations/buildings and electric vehicle chargers. These ac-dc converters with PFC must meet the standards and harmonic regulation requirements such as IEC 61000-3-2 and IEEE 519; and at the same time must achieve high power density at low cost of the system. In addition it must achieve high conversion efficiency with low input-current harmonics, good voltage regulation, and high PFC capability[1].

The Power Factor correction (PFC) is the major concern because if the number of electronic devices using smps increases, power from the grid varies the power factor of the supply which causes disturbance to the grid, Power-factor correction (PFC) is used to avoid the current harmonics of the input and thereby minimizing interference with other devices being powered from the same input source. Hence for each and every application a power factor corrector is required.

Power factor is defined as the ratio of power input to the product of r.m.s value voltage and current of the input.

$$\text{Power Factor} = \frac{P_i}{V_{rms} I_{rms}}$$

Development of efficient ac-dc converters with PFC has been the subject of considerable research. Single-stage ac-dc converters with PFC are considered attractive because they have high conversion efficiency, low cost, and less number of components [2-6]. However, they suffer less power factor (PF) and high voltage stress and they require a large dc link electrolytic capacitor and an inductor, which increases the size and cost of the converter. As another solution, single power conversion ac-dc converters with PFC have been introduced [7-9]; they do not require a large inductor or large dc-link electrolytic capacitor. They can achieve high PF under grid voltage variations. However, these single power-conversion ac-dc converters with PFC use bridge diodes on the input side of the rectifier, which causes high conduction losses and overheating of the components.

To overcome the problems of conventional converters Bridgeless converters have been introduced [10-17]. Firstly, bridgeless PFC boost rectifiers were proposed [10, 11]. Compared

to the conventional PFC boost rectifiers, these bridgeless PFC boost rectifiers increase the efficiency of the converter by eliminating the diodes and their forward-voltage drop. Furthermore, PFC boost rectifier output voltage is always greater than the peak of grid voltage, and therefore it cannot be used for low-voltage applications. To produce adjustable output voltages Bridgeless single-stage ac/dc converters have been proposed [12-16]. They help to reduce the number of components, but these bridgeless single-stage ac-dc converters are still large. Bridgeless flyback rectifier is presented to minimize the number of components [17]. It does not utilize bridge diodes, hence it does not suffer from diode conduction loss. However, Bridgeless flyback rectifier requires auxiliary circuits for proper operation. Also, the fly-back structure is usually restricted to low-power applications since it requires larger magnetic components for high-power applications. Moreover, in the flyback structure the usage of the transformer is poor and large transformer core is required to maintain the required power level.

This paper presents a high-efficiency bridgeless dual-mode single phase resonant ac-dc converter with pi controller. It is simple in structure and low in conduction loss since it uses a bidirectional switch instead of full bridge diodes. A series resonant circuit in the output voltage doubler on the secondary side. The series resonant circuit give zero-current switching (zcs) turn-off at the output diode, and consequently it reduces the reverse recovery loss.

To achieve medium-high power capacity with appropriate transformer, it operates in continuous conduction mode (CCM) when the instantaneous power level is high and is discontinuous conduction mode (DCM) when the instantaneous power level is low. The operating principle of the proposed converter are presented and simulation results are obtained.

## II. OPERATING PRINCIPLE

Fig. 1 shows the circuit diagram of the proposed bridgeless dual mode resonant single phase ac-dc converter. The bidirectional switch is used to transfer the energy to the secondary side without rectifying the input ac grid voltage. During the positive half cycle of the input voltage, the main switch S1 is turned on according to the duty-cycle. During the negative half-cycle of input voltage, switch S2 is turned on and acts as the main switch. S1 and S2 operates complementary to each another. When the bidirectional switch is turned on, the primary side energy is transferred to the secondary side through the series-resonant circuit. When the bidirectional switch is turned off, the energy which

is stored in mutual inductor ( $L_m$ ) is transferred to the secondary side. This enables the proposed bridgeless dual-mode single phase resonant ac-dc converter to process high power and high efficiency by using a single bidirectional switch.

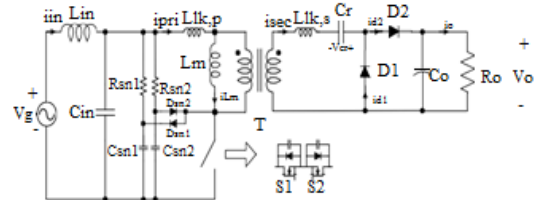


Fig. 1. Circuit diagram of bridgeless dual mode resonant single phase ac-dc converter.

Where, equivalent model parameters of the primary side switches;  $R_{sni}$ ,  $C_{sni}$ ,  $D_{sni}$  ( $i = 1, 2$ ): parameters of bidirectional RCD snubber;  $T$ : transformer with turns ratio  $n = N_s/N_p$ .  $L_m$ : magnetizing inductance;  $D1$ ,  $D2$ : secondary diodes;  $L_{lk,p}$ : primary leakage inductance;  $L_{lk,s}$ : secondary leakage inductance;  $C_r$ : resonant capacitor;  $R_o$ : output load.  $C_o$ : output capacitor;  $v_g$ : grid voltage;

The proposed converter is designed to operate in CCM when the instantaneous power level is high, and in DCM when the instantaneous power level is low. The proposed converter achieves high efficiency when it operates in CCM than when it operates in DCM. As the magnetizing inductance  $L_m$  increases, the CCM region widens, and thereby it increases the efficiency. However, large  $L_m$  requires large transformer size, so  $L_m$  must be selected appropriately. During CCM steady-state operation,  $T_s$  is divided into four operating modes. The equivalent circuit of each mode of operation are shown in Fig. 2.

Several assumptions are made to analyze the operation of the proposed converter:

- 1) The output capacitor  $C_o$  is large that the output voltage  $V_o$  is assumed to have no voltage ripple;
- 2) The grid voltage  $v_g$  is constant because the switching frequency  $f_s$  is much larger than the grid frequency  $f_g$ ;
- 3) The switch  $S1$  is modulated with duty ratio  $D$ , and the switch  $S2$  acts complementary to  $S1$  with short dead time.
- 4) The transformer  $T$  is ideal with the primary leakage inductance  $L_{lk,p}$ , the magnetizing inductance  $L_m$ , and the secondary leakage inductance  $L_{lk,s}$ ;

2.1 CCM Operation

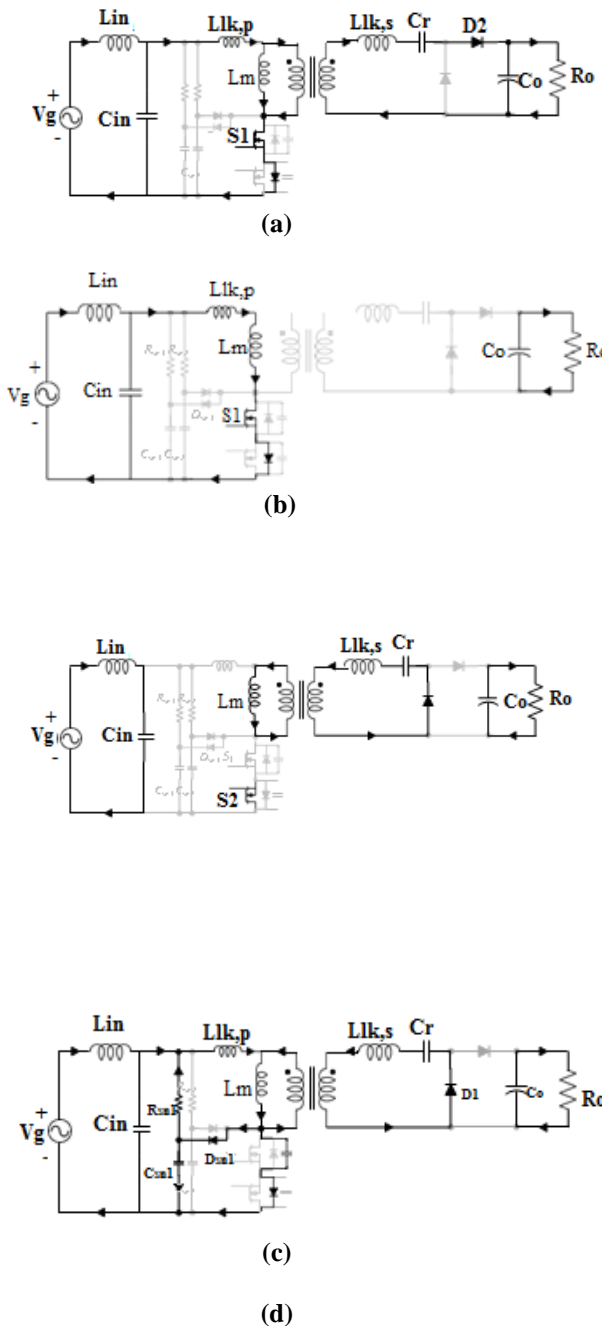


Fig. 2. Equivalent circuit of bridgeless resonant ac-dc converter when operates in CCM. (a) Mode 1. (b) Mode 2. (c) Mode 3. (d) Mode 4.

**Mode 1** [ $t_0, t_1$ ]: At time  $t_0$ , Switch  $S_1$  is turned on and the secondary current  $i_{sec}$  starts to resonate due to secondary leakage inductance  $L_{lk,s}$  and resonating capacitance  $C_r$  and it is directly transferred to the load through diode  $D_2$ . We considered  $V_{cin}$  as  $V_g$ ; during  $T_s$ ,  $V_g$  is considered to

be constant. Also, we assume  $L_m \gg L_{lk,p}$ . Then,  $i_{Lm}$  increases linearly as

$$\frac{di_{Lm}(t)}{dt} = \frac{V_g}{L_m} \quad (1)$$

During this interval, the power input is transferred to the output stage of the transformer and magnetic inductor  $L_m$  gets charged.

since,  $L_m \gg L_{lk,p}$ , The secondary side voltage  $V_{sec}$  of the transformer can be expressed as  $nV_g$ . The state equation of the circuit can be written as

$$L_{lk,s} \frac{di_{sec}(t)}{dt} = nV_g - V_o + v_{cr}(t), \quad (2)$$

$$i_{sec}(t) = -C_r \frac{dv_{cr}(t)}{dt} \quad (3)$$

with  $v_{cr}(t_0) = 0$ , where  $v_{cr}$  is the voltage across resonant capacitor  $C_r$ . Solving (2) and (3) yields

$$i_{sec}(t) = \frac{nV_g - (V_o - v_{cr}(t_0))}{Z_r} \sin[\omega_r(t - t_0)] \quad (4)$$

where the characteristic impedance  $Z_r$  and the resonant angular frequency  $\omega_r$  are given by

$$Z_r = \sqrt{\frac{L_{lk,s}}{C_r}}, \quad \omega_r = \frac{1}{\sqrt{L_{lk,s}C_r}}$$

At the same time, the power input charges magnetic inductor  $L_m$  and  $i_{Lm}$  is increased linearly as

$$i_{Lm}(t) = i_{Lm}(t_0) + \frac{V_g}{L_m}(t - t_0) \quad (5)$$

where  $i_{Lm}(t_0)$  is the initial value of  $i_{Lm}(t)$ .

**Mode 2** [ $t_1, t_2$ ]: At time  $t_1$ , the resonance between resonant capacitor  $C_r$  and secondary leakage inductance  $L_{lk,s}$  terminates and  $i_{sec}$  becomes zero. The diode  $D_2$  is turned off with zero current switching (zcs) and therefore the reverse-recovery loss does not occur. The power input charges the magnetic inductor  $L_m$  and  $i_{Lm}$  increases linearly as

$$i_{Lm}(t) = i_{Lm}(t_0) + \frac{V_g}{L_m}(t - t_0) \quad (6)$$

$$i_{sec}(t) = 0 \quad (7)$$

**Mode 3** [ $t_2, t_3$ ]: At time  $t_2$ , Switch  $S_1$  is turned off and magnetic inductor current  $i_{Lm}$  is transferred to the secondary side of the transformer. A high voltage spike occurs at the switch.

Here, the RCD snubber circuit absorbs the primary leakage inductor current  $i_{lk,p}$  by turning on the snubber diode whenever  $v_{ds}$  exceeds  $v_g + v_{cr}/n$ .

**Mode 4** [ $t_3, t_4$ ]: At  $t_3$  secondary current  $i_{sec}$  already begins to resonate due to mutual inductor  $L_m$  and resonant capacitor  $C_r$ .  $i_{Lm}(t_2)$  is reflected on the initial value of the secondary side

Then, the state equation of  $i_{sec}$  can be written as

$$i_{sec}(t) = -\frac{v_g}{nL_m}DT_s + \frac{V_{cr}}{n^2L_m}(t - t_2) \quad (8)$$

## 2.2 DCM operation

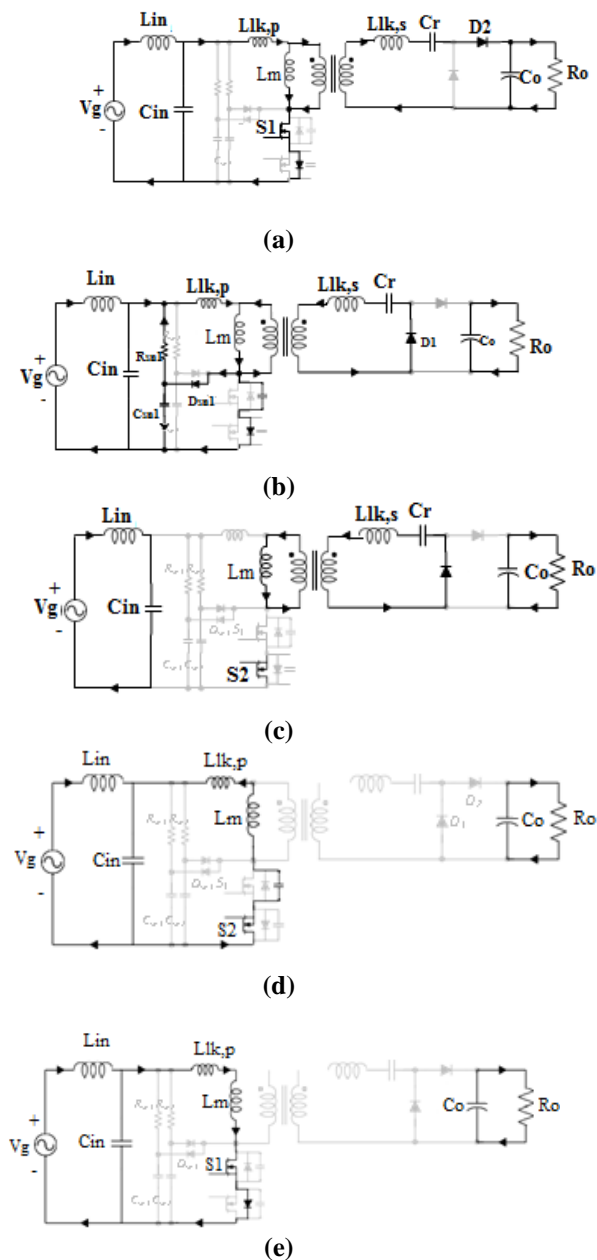


Fig. 2.1. Equivalent circuit of bridgeless resonant ac-dc converter when operates in DCM.

(a) Mode 1. (b) Mode 2. (c) Mode 3. (d) Mode 4.

**Mode 1 [t0, t1]:** At time t0, S1 is turned on and isec begins to flow through output diode D2. vg is approximately constant during Ts, isec becomes

$$i_{sec}(t) = \frac{nV_g - (V_o - V_{cr}(t_0))}{Z_r} \sin[\omega_r(t - t_0)] \quad (9)$$

At the same time, the input power charges magnetic inductor Lm and iLm increases linearly as

$$i_{Lm}(t) = \frac{V_g}{L_m} (t - t_0) \quad (10)$$

**Mode 2 [t1, t2]:** At time t1, the resonance between Cr and Llk,s terminates and isec becomes zero. Diode D2 is turned off with zero current and therefore reverse-recovery loss does not occur. The input power charges the magnetic inductor Lm and iLm increases linearly as

$$i_{Lm}(t) = i_{Lm}(t_1) + \frac{V_g}{L_m} (t - t_1) = \frac{V_g}{L_m} (t - t_0) \quad (11)$$

$$i_{sec}(t) = 0 \quad (12)$$

**Mode 3 [t2, t3]:** At time t2, Switch S1 is turned off and iLm is transferred to the secondary side. Similar to CCM operation, the RCD snubber circuit absorbs the primary leakage current.

**Mode 4 [t3, t4]:** Similar to isec in CCM, isec in DCM can be obtained as

$$i_{sec}(t) = -\frac{v_g}{nL_m} DT_s + \frac{V_{cr}}{n^2 L_m} (t - t_2) \quad (13)$$

**Mode 5 [t4, t5]:** At time t4, secondary current isec becomes zero. Diode D1 is turned off with zero current, and therefore reverse recovery loss does not occur. t4 can be calculated from (13) as

$$t_4 = t_2 + \frac{nv_g DT_s}{V_{cr}} \quad (14)$$

Since the secondary current isec becomes zero, the diode D1 is turned off. The residual energy in the circuit causes the resonance between CS1, magnetizing inductor Lm, and primary leakage inductance Llk,p, which generates the sinusoidal oscillation of vds in the interval t3 and t4. This oscillation is reflected to vD1.

## III. DESIGN OF PARAMETERS

### 3.1 Determining magnetizing inductance:

The proposed converter operates in CCM when  $v_g \geq v_{g,crit}$ , and in DCM when  $v_g \leq v_{g,crit}$ . The boundary between DCM and CCM is determined by magnetizing inductance Lm. Increase in Lm widens the CCM region, and increases the efficiency, but it increases the size of the converter. Thus, magnetizing inductance Lm must be chosen correctly.

### 3.2 Determining resonant capacitance:

To guarantee zero current switching (zcs) turn-off at diode D2, minimum turn-on time of the switch must be greater than the half of the resonant period or

$$\pi \sqrt{L_{lk,s} C_r} < D_{min} T_s \quad (15)$$

The minimum duty ratio is given as

$$D_{min} = 1 - \frac{\sqrt{2n} V_{g,rms}}{V_o} \quad (16)$$

From which

$$C_r < \frac{T_s^2}{\pi^2 L_{lk,s}} \left( 1 - \frac{\sqrt{2n} V_{g,rms}}{V_o} \right) \quad (17)$$

### 3.3 Selecting transformer turns ratio:

The turns ratio n of the transformer can be selected from the voltage gain of the converter.

$$n \leq \frac{V_o}{\sqrt{2}V_{grms}} \quad (18)$$

### 3.4 Determining output capacitance:

To satisfy the output voltage ripple, we select the output capacitor as

$$C_o \geq \frac{P_o}{2\pi f_g V_o \Delta V_o} \quad (19)$$

where  $\Delta V_o$ -output voltage ripple.

## IV. SIMULATION RESULTS:

The proposed bridgeless dual mode resonant single phase ac-dc converter, simulation was performed using MATLAB/SIMULINK with grid voltage  $V_g=120-220$  V. To satisfy Zero current switching (ZCS) turn-off at output diode D2 over the entire grid period, resonant capacitance ( $C_r$ ) is set to  $4.4 \mu F$ . considering the cost of the converter, magnetizing inductance ( $L_m$ ) was set to  $300 \mu H$ .

The simulation of proposed converter is as shown in fig. 3.1. The selected specific components (Table I) were the same as in the simulation.

**Table I**  
**PARAMETERS AND VALUES OF COMPONENTS.**

Parameters	Symbols	Value
Grid voltage	vg	120–220 V
Output voltage	$V_o$	330V
Switching frequency	fs	50 kHz
Primary capacitor	$C_{in}$	$6.6 \mu F$
Primary inductor	$L_{in}$	$940 \mu H$
Magnetizing inductance	$L_m$	$300 \mu H$
Primary leakage inductance	$L_{lk,p}$	$1.39 \mu H$
Secondary leakage inductance	$L_{lk,s}$	$0.86 \mu H$
Snubber resistance	$R_{sn1}, R_{sn2}$	200 k $\Omega$
Snubber capacitance	$C_{sn1}, C_{sn2}$	22 nF
Output capacitance	$C_o$	$1320 \mu F$
Resonant capacitance	$C_r$	$4.4 \mu F$

During CCM, ZCS turn-off is guaranteed at output Diode D2. The input current was almost sinusoidal. Input current  $i_{in}$  was synchronized with grid voltage  $v_g$ .

## 4.1 simulation of proposed converter

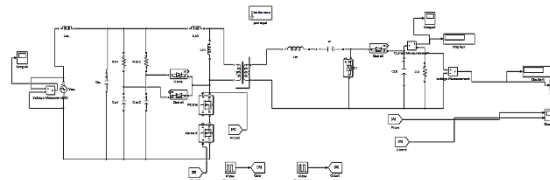


**Fig. 4.1. Simulation of proposed converter.**

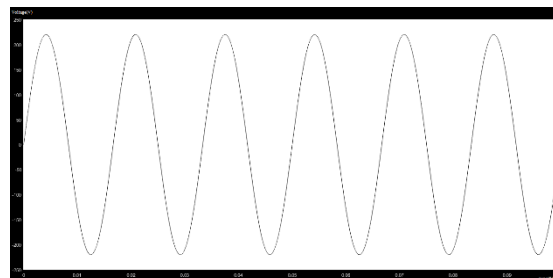


**Fig. 4.2. Input voltage waveform  $V_{in}=220V$ .**

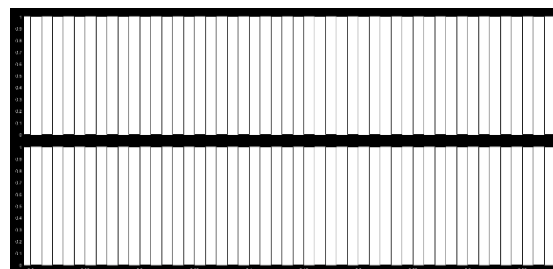


**Fig. 4.3. Gate pulses to switch S1 and S2.**

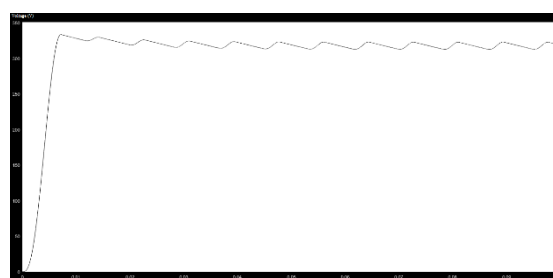


**Fig. 4.4. Output Voltage.**

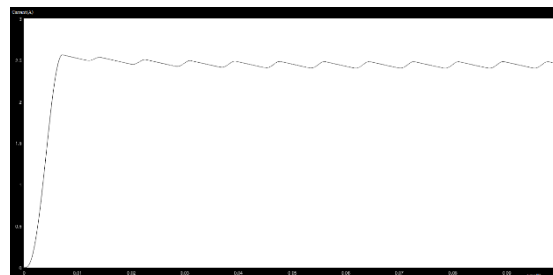


**Fig. 4.5. Output current.**

The output voltage equation is given by:

$$V_o = V_g n(D + 1)(20)$$

$$V_o = 220 * 1 * (0.5 + 1)$$

$$V_o = 330 \text{ V (Theoretical value)}$$

By simulation

$$V_o = 318.2 \text{ V}$$

The output voltage obtained in open loop simulation is  $V_o = 330 \text{ V}$ . This discrepancy is because of the semiconductor devices (diode and switch) voltage drop when they are made on.

Output power is given by:

$$P_o = V_o * I_o$$

$$P_o = 318.2 * 2.448$$

$$P_o = 778.9 \text{ W}$$

Power obtained in open loop simulation is 778.9W which is less than required value hence we go for closed loop circuit with PI controller.

#### 4.1.1 Simulation of proposed converter with pi controller.

##### 4.1.1.1 Block diagram of converter with pi controller

The output of the proposed high-efficiency bridgeless dual-mode single phase resonant ac-dc converter is not constant because of the difference in the environmental condition therefore it requires control techniques. Hence to obtain the required output voltage to meet the load demand, closed loop control with proportional integral (PI) controller is employed. The block diagram shown in figure 4.1.1 explains the implementation of proportional integral (pi) controller for high-efficiency bridgeless dual-mode single phase resonant ac-dc converter. The actual output voltage of the high-efficiency bridgeless dual-mode single phase resonant ac-dc converter and the constant reference signal are compared, to obtain a error signal (e). The error signal (e) is given to proportional integral (pi) controller. The pi controller generates the control signal based on error signal for varying the turn on and turn off time of the switch of the bridgeless dual-mode single phase resonant ac-dc converter, to maintain constant output voltage ( $V_o$ ) irrespective of the variation in load and input voltage. Similarly to maintain constant output current pi controller is used.

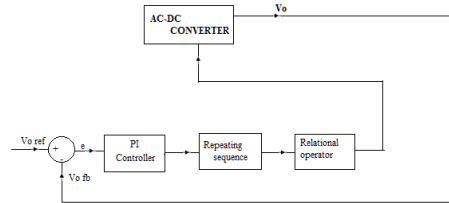


Fig. 4.1.1. Block diagram of proposed converter with pi controller for voltage control.

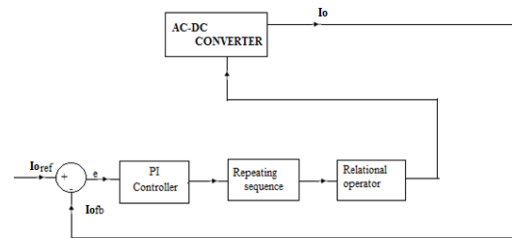


Fig. 4.1.2. Block diagram of proposed converter with pi controller for current control.

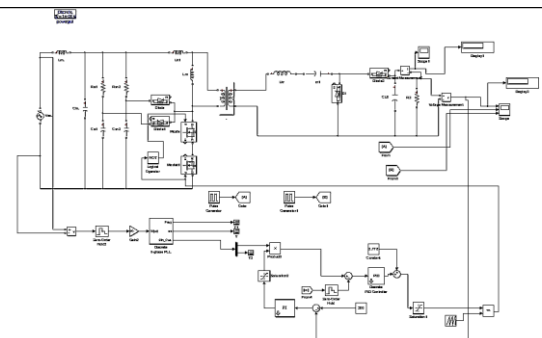


Fig. 4.1.3 Simulink of proposed converter with pi controller.

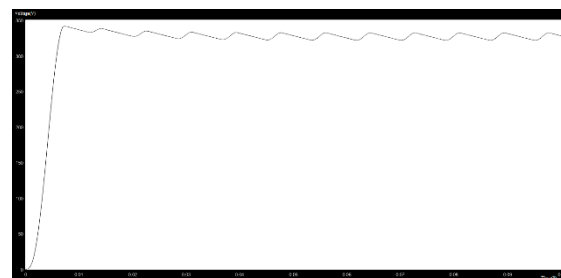


Fig. 4.1.4. Output voltage with pi controller when  $V_i = 220 \text{ V}$ ,  $V_o = 330 \text{ V}$ .

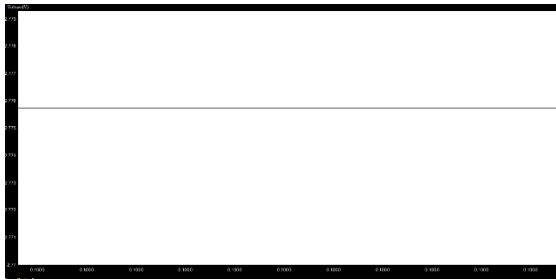


Fig. 4.1.5. Output current with pi controller when  $V_i=220V$ ,  $I_o=2.73A$ .

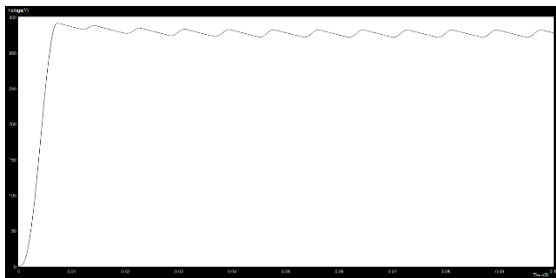


Fig. 4.1.6. Output voltage with pi controller when  $V_i = 215V$ ,  $V_o = 330V$ .



Fig. 4.1.7. Output current with pi controller when  $V_i = 215V$ ,  $I_o = 2.73A$ .

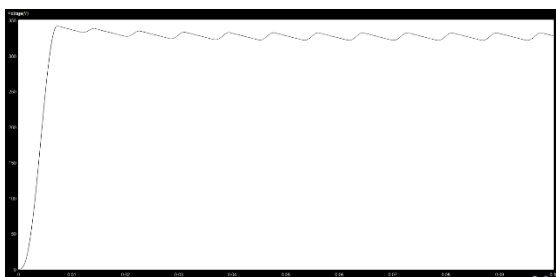


Fig. 4.1.8. Output voltage with pi controller when  $V_i = 225V$ ,  $V_o = 330V$ .



Fig. 4.1.9. Output current with pi controller when  $V_i = 225V$ ,  $I_o = 2.73A$ .

With pi controller

$$V_o = 330 V$$

$$P_o = V_o * I_o$$

$$P_o = 330 * 2.73$$

$$P_o = 900W$$

Power obtained in closed loop simulation with pi controller is 900W which is the required power level.

$$\text{Efficiency} = \frac{P_o}{P_i}$$

$$\text{Efficiency} = \frac{900}{935} = 96.2\%$$

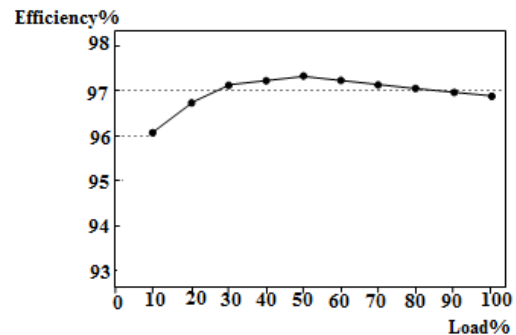


Fig. 4.1.10. Efficiency of proposed converter when  $V_i=220V$ .

Remark 1. The proposed converter operates similar to the forward converter and during the half switching period it transfers the energy to the load in resonant way. Then, during the other half switching period the proposed converter transfers the magnetizing energy in the transformer to the series resonant circuit.

Remark 2. The applications of the converter are common dc-bus suppliers in buildings/mobile charging stations [23]. It can also be used as level-2 battery charger by connecting the proposed converters in parallel [24]. Furthermore, it can be used in high voltage applications such as traveling wave tubes, medical X-ray imaging, and lasers [25].

## V. CONCLUSION

This paper presents a high-efficiency bridgeless dual-mode single phase resonant ac-dc converter. To reduce the number of components, the grid-side full-bridge diode rectifier is expelled and is replaced by a single bidirectional switch; as a result, the primary side conduction loss and number of components and size and cost were reduced. Use of a series-resonant voltage-doubler structure reduced the cost of the proposed converter and enables its use in medium-high power applications. Moreover the proposed converter achieves accurate output voltage regulation and high efficiency. To confirm the validity of the proposed converter, open loop and closed loop simulation was performed.

## REFERENCES

- [1]. 80 Plus Incentive Program. [Online]. Available: <http://www.80plus.org>
- [2]. M. Narimani and G. Moschopoulos, "A new interleaved three-phase single-stage PFC AC-DC converter with flying capacitor," *IEEE Trans. Power Electron.*, vol. 30, no. 7, pp. 3695-3702, Jul. 2015.
- [3]. B. Poorali and E. Adib, "Analysis of the integrated SEPIC flyback converter as a single-stage single-switch power-factor correction LED driver," *IEEE Trans. Ind. Electron.*, vol. 63, no. 6, pp. 3562-3570, Jun. 2016.
- [4]. H. Ma, J. S. J. Lai, C. Zheng, and P. Sun, "A high-efficiency quasi-single-stage bridgeless electrolytic capacitor-free high power AC-DC driver for supplying multiple LED strings in parallel," *IEEE Trans. Power Electron.*, vol. 31, no. 8, pp. 5825-5836, Aug. 2016.
- [5]. P. Fang and Y. F. Liu, "Energy channeling LED driver technology to achieve flicker-free operation with true single stage power factor correction," *IEEE Trans. Power Electron.*, vol. 32, no. 5, pp. 3892-3907, May 2017.
- [6]. S. Li, W. Qi, S. C. Tan, and S. R. Hui, "A single-stage two-switch PFC rectifier with automatic AC ripple power decoupling and wide output voltage range," *IEEE Trans. Power Electron.*, vol. 32, no. 9, pp. 6971-6982, Sep. 2017.
- [7]. S. Li, W. Qi, S. C. Tan, and S. R. Hui, "A single-stage two-switch PFC rectifier with wide output voltage range and automatic AC ripple power decoupling," *IEEE Trans. Power Electron.*, vol. 32, no. 9, pp. 6971-6982, Sep. 2017.
- [8]. Y. W. Cho, J. M. Kwon, and B. H. Kwon, "Single power conversion AC-DC converter with high power factor and high efficiency," *IEEE Trans. Power Electron.*, vol. 29, no. 9, pp. 4797-4806, Sep. 2014.
- [9]. S. G. Jeong, W. J. Cha, S. H. Lee, J. M. Kwon, and B. H. Kwon, "Electrolytic capacitor-less single-power-conversion onboard charger with high efficiency," *IEEE Trans. Ind. Electron.*, vol. 63, no. 12, pp. 7488-7497, Dec. 2016.
- [10]. K. S. Kim, J. M. Kwon, and B. H. Kwon, "Single-switch single power-conversion PFC converter using regenerative snubber," *IEEE Trans. Ind. Electron.*, vol. 65, no. 7, pp. 5436-5444, Jul. 2018.
- [11]. L. Huber, Y. Jang, and M. M. Jovanovic, "Performance evaluation of bridgeless PFC boost rectifiers," *IEEE Trans. Power Electron.*, vol. 23, no. 3, pp. 1381-1390, Mar. 2008.
- [12]. B. Su, J. Zhang, and Z. Lu, "Totem-pole boost bridgeless PFC rectifier with simple zero-current detection and full-range ZVS operating at the boundary of DCM/CCM," *IEEE Trans. Power Electron.*, vol. 26, no. 2, pp. 427-435, Feb. 2011.
- [13]. W. Y. Choi and J. S. Yoo, "A bridgeless single-stage half-bridge AC/DC converter," *IEEE Trans. Power Electron.*, vol. 26, no. 12, pp. 3884-3895, Dec. 2011.
- [14]. S. W. Lee and H. L. Do, "Single-stage bridgeless ac-dc PFC converter using a lossless passive snubber and valley switching," *IEEE Trans. Ind. Electron.*, vol. 63, no. 10, pp. 6055-6063, Oct. 2016.
- [15]. M. Alam, W. Eberle, D. S. Gautam, C. Botting, N. Dohmeier, and F. Musavi, "A hybrid resonant pulse-width modulation bridgeless AC-DC power factor correction converter," *IEEE Trans. Ind. Appl.*, vol. 53, no. 2, pp. 1406-1415, Feb. 2017.
- [16]. A. Malschitzky, F. Albuquerque, E. Agostini, and C. B. Nascimento, "Single-stage integrated bridgeless-boost nonresonant half-bridge converter for LED driver applications," *IEEE Trans. Ind. Electron.*, vol. 65, no. 5, pp. 3866-3878, May 2018.
- [17]. H. Ma, Y. Li, J. S. Lai, C. Zheng, and J. Xu, "An improved bridgeless SEPIC converter without circulating losses and input voltage sensing," *IEEE Trans. Emerg. Sel. Topics Power Electron.*, vol. 6, no. 3, pp. 1447 - 1455, Sep. 2018.
- [18]. J. W. Shin, S. J. Choi, and B. H. Cho, "High-efficiency bridgeless flyback rectifier

- with bidirectional switch and dual output windings,” *IEEE Trans. Power Electron.*, vol. 29, no. 9, pp. 4752-4762, Sep. 2014.
- [19]. E. H. Kim and B. H. Kwon, “Zero-voltage-and zero-currentswitching full-bridge converter with secondary resonance,” *IEEE Trans. Ind. Electron.*, vol. 57, no. 3, pp. 1017-1025, Mar. 2010.
- [20]. S. Kim, B. Kim, B. H. Kwon, and M. Kim, “An active voltagedoubler rectifier based hybrid resonant DC/DC converter for wide-input-rangethermo-electricpowergeneration,” *IEEE Trans. Power Electron.*, vol. 33, no. 11, pp. 9470-9481, Nov. 2018.
- [21]. S Monica, Dr Usha P, “Closed Loop Control of Single Phase Bridgeless Resonant AC-DC Converter” *ijera*, vol.10, issue 7, (series-7) july 2020.
- [22]. H. Kim, J. S. Lee, J. S. Lai, and M. Kim, “Iterative learning controller with multiple phase-lead compensation for dual-mode flyback inverter,” *IEEE Trans. Power Electron.*, vol. 32, no. 8, pp. 6468-6480, Aug. 2017.
- [23]. B. Han, J. S. Lai, and M. Kim, “Dynamic modeling and controller design of dual-mode Cuk inverter in grid-connected PV/TE Applications,” *IEEE Trans. Power Electron.*, vol. 33, no. 10, pp. 8887-8904, Oct. 2018.
- [24]. Y. Cho and J. S. Lai, “Digital plug-in repetitive controller for single-phase bridgeless PFC converters,” *IEEE Trans. Power Electron.*, vol. 28, no. 1, pp. 165-175, Jan. 2013.
- [25]. C. Wang, X. Li, L. Guo, and Y. W. Li, “A nonlinear-disturbanceobserver-based DC-bus voltage control for a hybrid AC/DC microgrid,” *IEEE Trans. on Power Electron.*, vol. 29, no. 11, pp. 6162-6177, Nov. 2014.
- [26]. M. Pahlevani and P. Jain, “A fast DC-bus voltage controller for bidirectional single-phase AC/DC converters,” *IEEE Trans. on Power Electron.*, vol. 30, no. 8, pp. 4536-4547, Aug. 2015.
- [27]. J. F. Chen, R. Y. Chen, and T. J. Liang, “Study and implementation of a single-stage current-fed boost PFC converter with ZCS for high voltage applications,” *IEEE Trans. on Power Electron.*, vol. 23, no. 1, pp. 379-386, Jan. 2008.